ACS APPLIED MATERIALS & INTERFACES

Research Article

www.acsami.org

Floating Growth of Large-Scale Freestanding TiO_2 Nanorod Films at the Gas–Liquid Interface for Additive-Free Li-Ion Battery Applications

Hua-Rong Xia,[†,‡] Jia Li,[†,§] Chen Peng,[†,⊥] Wen-Tao Sun,*[,†,‡,⊥] Long-Wei Li,[†,‡] and Lian-Mao Peng*[,†,‡,§]

[†]Key Laboratory for the Physics and Chemistry of Nanodevices, [‡]Department of Electronics, [⊥]School of Software and Microelectronics, [§]Academy for Advanced Interdisciplinary Studies, Peking University, Beijing 100871, China

Supporting Information

ABSTRACT: The floating growth process of large-scale freestanding TiO_2 nanorod films at the gas–liquid interface was investigated. On the basis of the experiments, a self-templated growth scenario was developed to account for the self-assembly process. In the scenario, titanium complexes function not only as the Ti source for the growth of TiO_2 but also as a soft template provider for the floating growth. According to the scenario, several new recipes of preparing freestanding TiO_2 nanorod films at the gas–liquid interface were developed. The freestanding film was applied to a lithium ion battery as a binder-free and conducting agent-free anode, and good cyclability was obtained. This work may pave a new way to floating and freestanding TiO_2 and other semiconductor materials, which has great potential not only in basic science but also in the applications such as materials engineering, Li-ion battery, photocatalyst, dye-sensitized solar cell, and flexible electronics.

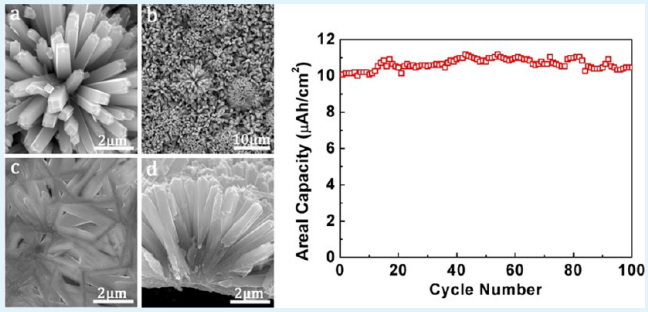

KEYWORDS: *self-templated, floating, freestanding, gas–liquid interface, binder-free, Li-ion battery*

1. INTRODUCTION

Freestanding two-dimensional (2D) nanostructures have attracted an ever-growing interest for their potential applications in the fields such as flexible electronics because the freestanding film can be readily transferred onto arbitrary substrates including flexible ones.[1] As one of the most promising semiconductors, titanium dioxide (TiO_2) has many potential applications such as photovoltaic, photocatalysis, catalyst support, gas sensor, Li-ion battery, and so on, because of its outstanding physical and chemical properties besides its environment-friendly, low-cost advantages.[2−10] Therefore, the synthesis of freestanding TiO_2 is of great interest and several methods for the fabrication of freestanding TiO_2 have been developed.[11−14] Most of them involve chemical selective etching of sacrificial layers, which usually consists of two steps, the synthesis of the film on substrates and the following detachment from them.[8−11] Few methods without the etching process have been developed,[15−17] including vessel bottom-assisted[15,16] or glass substrate-assisted[17] method. However, in all of these methods, the freestanding film was synthesized at the solid–liquid interface and the separation of the film from the solid substrate or the wall of vessel is essential, which makes it very hard to obtain large-scale continuous substrate-free film.[12−14] Most recently, we reported a one-step substrate-free synthesis of large-scale floating TiO_2 nanorod films at the gas–liquid interface, which offered a new method of synthesizing freestanding TiO_2 nanorod films.[18,19]

In this paper, the floating growth process of the freestanding nanorod films at the gas–liquid interface was investigated. Based on the process, a self-templated growth scenario was developed, in which the titanium complexes act as a soft template provider for the floating growth besides the commonly reported role of Ti source. According to the scenario, several other recipes of preparing freestanding TiO_2 films were developed, which further verified the scenario. Furthermore, the freestanding film was applied to a lithium ion battery as an anode without binder and conducting agent with good cyclability obtained. To the best of our knowledge, it was the first time that a binder-free and conducting agent-free TiO_2 anode was applied to lithium ion battery with good cyclability. This work has great potential not only in basic science but also in fields such as materials engineering, Li-ion batteries, photocatalysts, dye-sensitized solar cells, flexible electronics, and so on.

Received: December 19, 2013
Accepted: September 22, 2014
Published: September 22, 2014

2. EXPERIMENTAL SECTION

2.1. Materials. Tetrabutyl titanate (TBT, Chemical Pure) was obtained from Beijing Yili Fine Chemical Co., Ltd. Concentrated hydrochloric acid (HCl, Analytical Reagent) was obtained from Beijing Chemical Works; fluorine-doped tin oxide (FTO) coated glass from Heptachroma, Dalian, China and Titanium tetrachloride ($TiCl_4$, Analytical Reagent) from Sinopharm Chemical Reagent Co., Ltd. Beijing, China. All reagents were used without further purification.

2.2. Film Synthesis. In a typical synthesis, 20 mL of deionized (DI) water was mixed with 20 mL of concentrated hydrochloric acid (36.5−38 wt %) in a weighing bottle (3.5 cm in diameter, 7 cm in height) first. Then 100−200 μL of $TiCl_4$ and 0.5−1 mL of TBT was added dropwise into the solution. After that, the weighing bottle was put into the Teflon-lined stainless steel autoclave (100 mL volume, Beijing STWY Equipment Co., Ltd.). The hydrothermal reaction was conducted at 150−160 °C for 1−24 h in an electric oven. After the reaction, the autoclave was naturally cooled to room temperature. The obtained film on the surface of the solution was took out with a piece of glass slide, rinsed with deionized water and dried in ambient air.

2.3. Device Fabrication. The freestanding film was first punched into circular films with the diameter of 14 mm, which were directly used as Cathode in CR2032 coin-type cells without the addition of binder or conducting agent. A circular Li foil with the diameter of 16 mm was used as the anode and 1 M $LiPF_6$ dissolved in a mixture of ethylene carbonate (EC), dimethyl carbonate (DMC) and ethyl methyl carbonate (EMC) with a volume ratio of 1:1:1 was used as electrolyte here. The separator is a microporous polypropylene membrane Celguard 2400. The cells were assembled in an argon protected glovebox with water and oxygen content less than 1 ppm.

2.4. Characterization. The morphology of the TiO_2 was characterized by a field-emission gun FEI Quanta 600F scanning electron microscope (SEM) and a FEI Tecnai F30 transmission electron microscope (TEM). A Rigaku D/max-rA 12 kW X-ray diffraction (XRD) system is used to test the structure with the Cu−Kα line with λ = 1.54 Å used as the source. A LAND CT2001A 8-channel automatic battery test system (Wuhan Jinnuo Electronics Co., Ltd.) is used to carry out constant current charging/discharging of the coin cells in a voltage range of 1.0−3.0 V. Cyclic voltammogram (CV) curve between 1 and 3 V was measured with a CHI 660C electrochemical station at a scan rate of 2 mV/s.[20]

3. RESULTS AND DISCUSSION

3.1. Characterization of the Film. The films directly grown at the gas−liquid interface were characterized by SEM. Figure 1 are SEM images, and the corresponding photographs are shown in Figure S1 in the Supporting Information, SI. Figure 1a and b is bottom view SEM pictures (seen from the liquid side), showing that the film is built up with nanorod-based flowerlike nanostructures. While Figure 1c is top view SEM picture (seen from the gas side), showing that the film is built up with lying nanorods. The sectional view of the film is shown in Figure 1d, which indicates that the microflower is composed of nanorods with one end interconnected. Closer observations are investigated by TEM. As shown in Figure 2a and b, many nanoparticles can be seen at the root of the microflowers. Figure 2c is a high-resolution image of one nanorod. The 0.32 nm of the interplanar spacing is corresponding to the (110) plane of the rutile TiO_2, which indicates that the nanorod grows along [001] direction. The corresponding SAED (selected area electron diffraction) result shown in Figure 2d is consistent with it. To confirm the crystalline structure, XRD experiments are carried out and the corresponding XRD pattern (Figure S2, SI) also indicates the film is rutile.

To investigate the formation mechanism of the floating film, there were two things needed to do. One is observing the growth process of the film at the gas−liquid interface; and the other is clarifying the important roles of various reactants in the process.

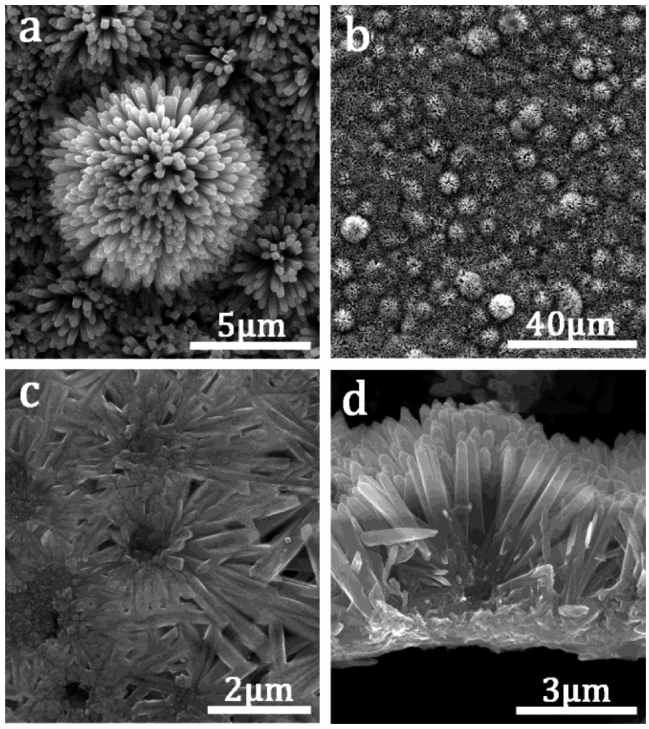

Figure 1. Typical SEM images of the film grown at the gas−liquid interface: (a, b) Bottom view of the film (seen from the liquid side). (c) Top view of the film (seen from the gas side). (d) The cross section of the film.

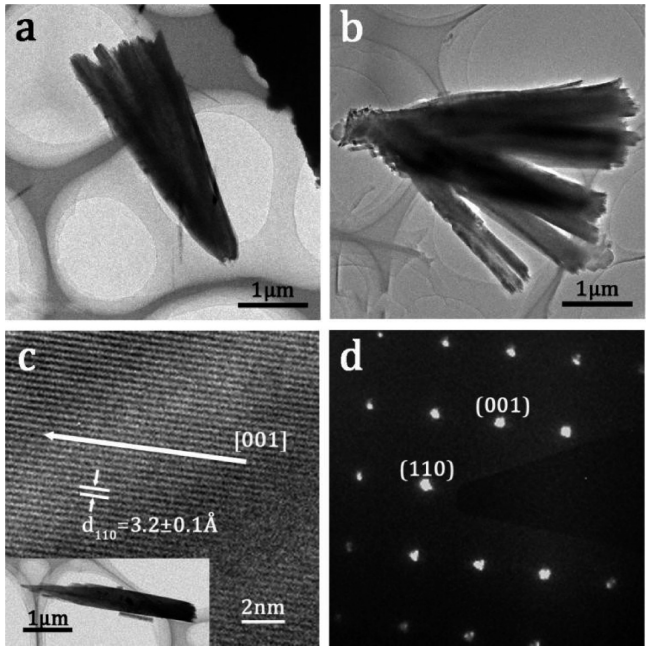

Figure 2. TEM characterization of the film: (a, b) TEM and (c) high-resolution TEM images of the film and the inset is the corresponding nanorod. (d) Selected area electron diffraction of the nanorod.

3.2. Growth Process of the Floating Film. To observe the growth process of the floating film, the reaction experiments for 1 to 6 h have been carried out. Figure 3

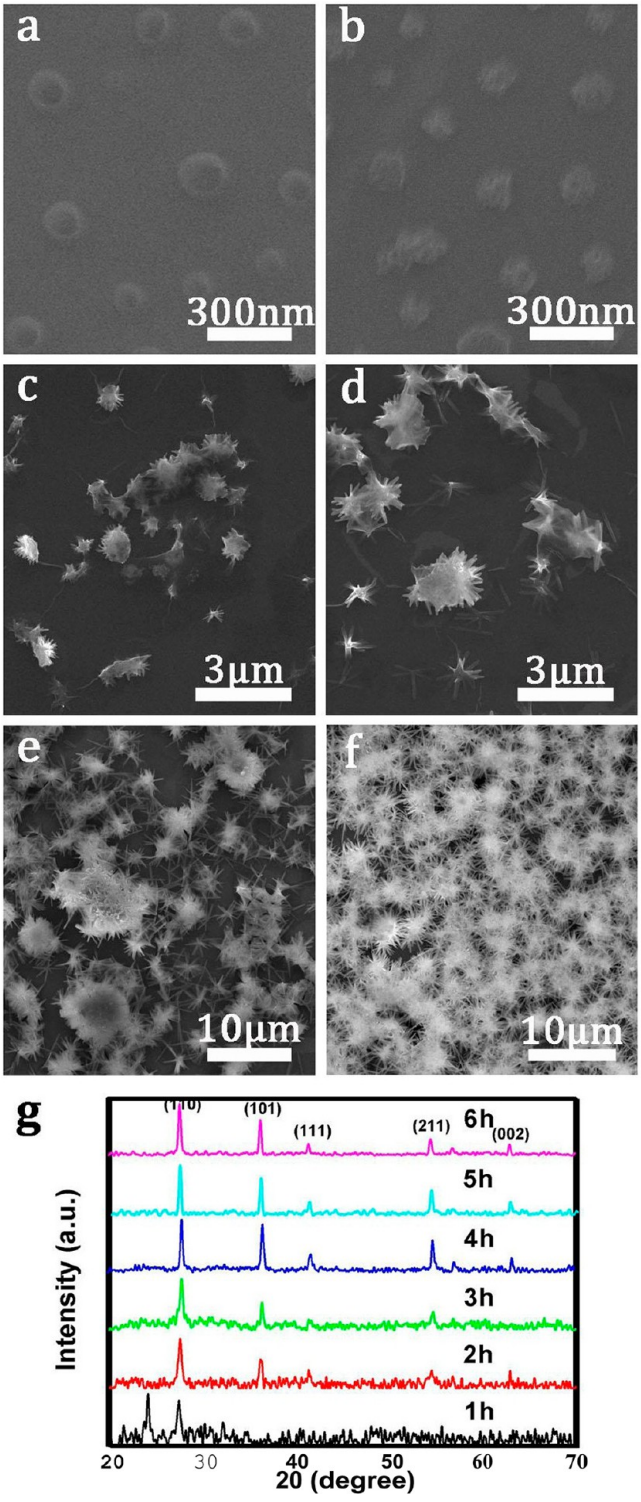

Figure 3. (a–f) SEM images and (g) XRD patterns of the reaction products obtained at the gas–liquid interface grown for 1–6 h (seen from the gas side).

shows typical SEM images of the reaction products at the gas–liquid interface which were scooped onto a Si wafer and the corresponding XRD patterns. Figure 3a is a SEM image of the sample reacted for 1 h, showing some clusters formed at the gas–liquid interface. Figure 3b and c is SEM images of the sample reacted for 2 and 3 h, suggesting that the nanorods started to grow out of the clusters. After reacted for 4 h, the

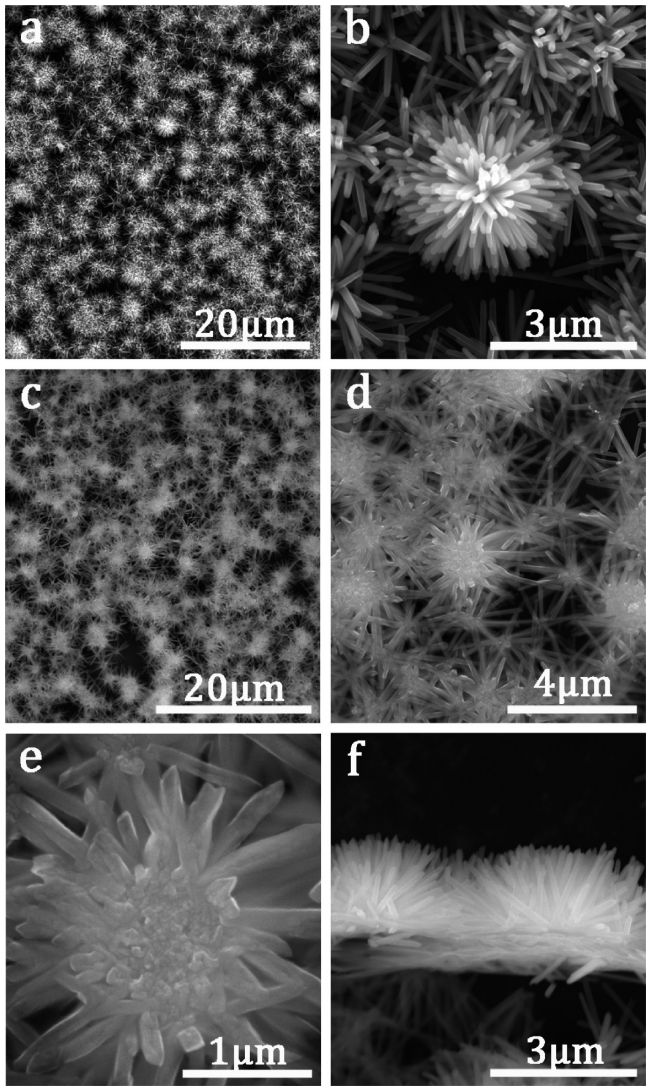

Figure 4. SEM images of the film grown at the gas–liquid interface for 6 h: (a, b) Bottom view (seen from the liquid side) of the film. (c–e) Top view (seen from the gas side) of the film. (f) Cross-sectional view of the film.

sample grew into flowerlike hierarchical structures (shown in Figure 3d), and grew larger and larger as the reaction proceeded. Then the flowerlike structures started to interconnect with each other so that the film began to form though it might be thin and unstable when it reacted for 5 h (Figure 3e). Finally, after the film grew for 6 h, the film changed to be thicker and stable enough to transfer (Figure 3f). The corresponding XRD patterns of the films grown for 1–6 h are shown in Figure 3g. Most of the diffraction peaks can be ascribed to rutile phase TiO_2 (JCPDS file No. 65-0192) except for the diffraction peak (2θ = 24.22°) in the pattern of the film reacted for 1 h, which may be ascribed to titanium hydrogen oxide hydrates, such as $H_2Ti_4O_9{\cdot}H_2O$ (JCPDS file No. 36–0655), that resulted from the hydrolysis of TBT. When the reaction was carried out over 1 h, the intermediates such as $H_2Ti_4O_9{\cdot}H_2O$ changed into TiO_2, so there were only diffraction peaks of TiO_2 in the reaction products for 2–6 h.

More SEM images of the film grown for 6 h are shown in Figure 4. It was noticed that the obtained film after 6 h reaction was similar to the film obtained from the reaction after 24 h

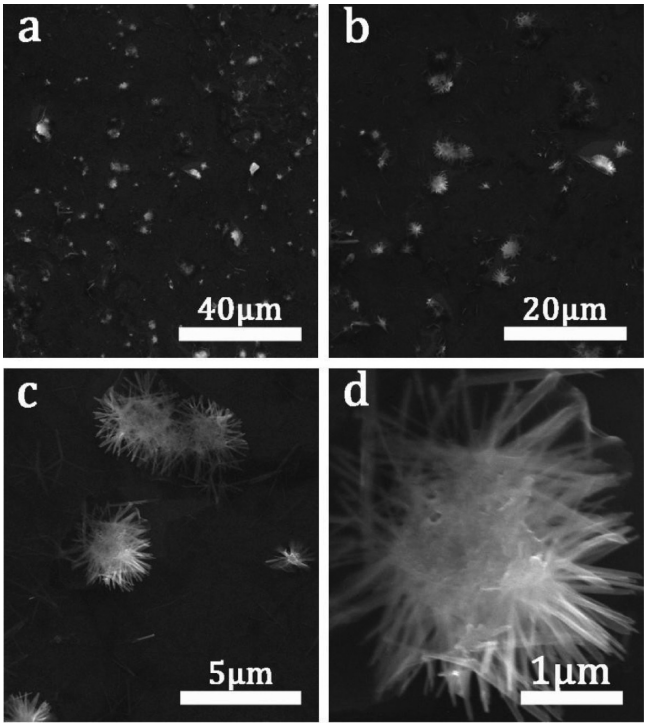

Figure 5. SEM images of floating TiO_2 without the addition of $TiCl_4$ grown for 12 h with different magnifications (a–d).

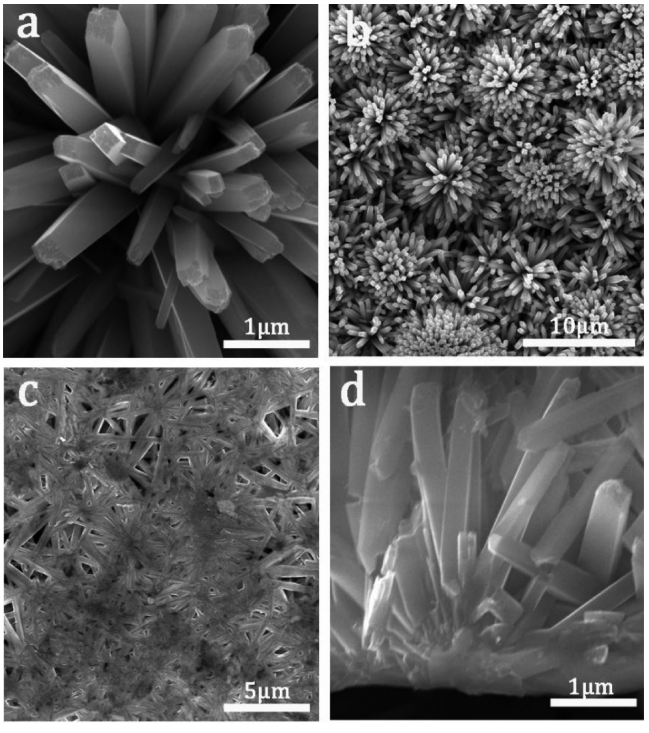

Figure 6. SEM images of the flowerlike film using FTO nanoparticles as seeds (a, b) Bottom view of the film seen from the liquid side. (c) Top view of the film seen from the gas side. (d) The cross section of the film.

(shown in Figure 1), which is composed of semispherical flowerlike nanostructures with one side of the film plane while the other side uneven. The main reason is that only the solution side can offer enough Ti source for the growth of the nanorods while the air side cannot.

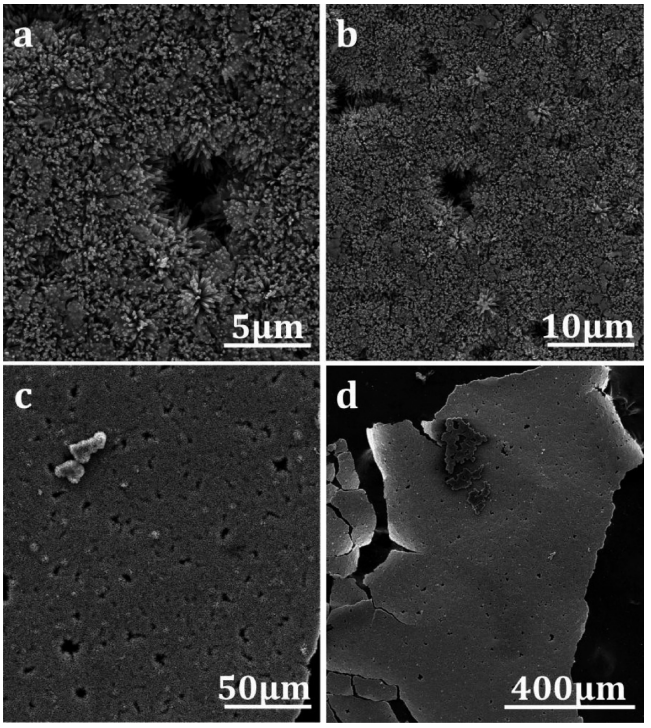

Figure 7. SEM images of the floating TiO_2 film with the addition of C_4H_9OH: (a–c) Bottom view of the film seen from the liquid side with different magnifications. (d) Top view of the film seen from the gas side.

Scheme 1. Illustration of the Scenario for Floating Growth of TiO_2 Nanorod Films at the Gas–Liquid Interface

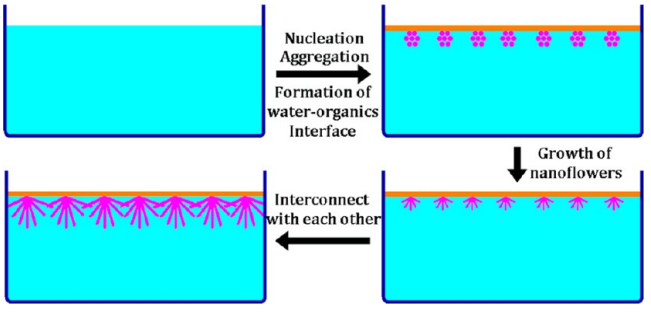

Table 1. Summary of the Experimental Results

no.	seed provider	Ti source/ template	results
A	$TiCl_4$	TBT	floating flowerlike film (Figure 1)
B1		TBT	floating flowerlike structures (Figure 5)
B2	FTO nanocrystals	TBT	floating flowerlike film (Figure 6)
C1	$TiCl_4$		nothing floating
C2	$TiCl_4$	butanol	floating flowerlike film (Figure 7)
C3	$TiCl_4$	ethanol/acetone/ ether	floating flowerlike structures
D1	$TiCl_4$	TET	floating flowerlike film (SI Figure S3)
D2	FTO nanocrystals	TET	floating flowerlike film (SI Figure S4)

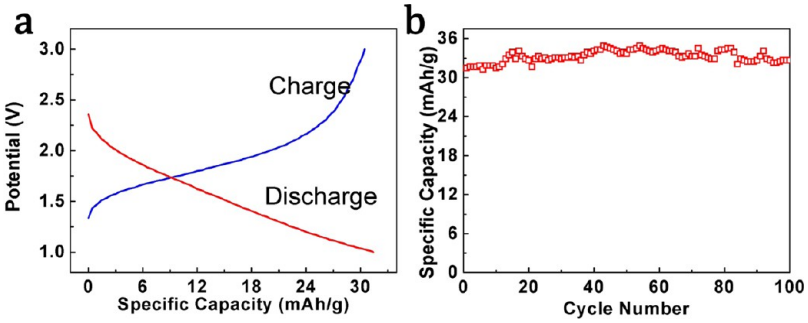

Figure 8. (a) Typical initial charge−discharge curves of the Li-ion battery using the freestanding TiO_2 film as binder-free and conducting agent-free anode. (b) The corresponding cycle performance of the same battery.

To understand the floating growth process of the film, there are two key questions to answer: one is how the TiO_2 grows into flowerlike structure; the other is why the film can achieve floating growth.

For the first question, there are many scenarios developed to account for the formation of flowerlike nanostructures.[21−24] Generally, it contains the following three steps: nucleation, aggregation, and growth, which can also be applied to the process here. At the first stage, the $TiCl_4$ hydrolyzes fast and nucleates to generate nanocrystals, which can be used as the seeds for the growth of the nanorods. The hydrolysis of the $TiCl_4$ solution can be expressed as the following reaction:[25]

$$Ti^{4+} + 2H_2O \leftrightarrow TiO_2 + 4H^+$$

Indeed, there are many reports about the formation of nanocrystals at the early stage of hydrothermal preparation of rutile nanorods.[26−29] As the process continues, the precipitates collide with each other due to forces such as electrostatic force, van der Waals force and so on, thereby resulting in the formation of aggregates as shown in Figure 3a and b.[25] At the second stage, nanorods begin to grow out of the clusters because the selective adsorption of Cl^- on the (110) plane of rutile TiO_2 nanocrystals guides anisotropic one-dimensional growth along the [001] orientation and generates nanorods.[24,30]As the air side cannot offer titanium source for the growth of nanorods, only that at the solution side nanorods could continue to grow and form the semispherical flowerlike hierarchical nanostructures as shown in Figure 3c and d. At the third stage, the nanorods grow longer and interconnect with each other to assemble into a film as shown in Figure 3e and f. In this way, the observed formation process of the flowerlike structures can be clarified according to the reported scenarios.[21−24] However, to the best of our knowledge, the floating growth process has not been understood. Clarifying the roles of various reactants in the floating growth seems to be necessary to explain it.

3.3. Roles of Various Reactants. To clarify different roles of the reactants in the floating growth process, an "exclusion-substitution" method was developed. To investigate the role of a reactant in the reaction, it was excluded from the reaction and the changes were observed to infer the possible role of the reactant, which was called the "exclusion" step. Then the reactant under study was substituted for another reactant with the same number of moles to play the same role as inferred above to verify whether the inference was correct or not, which was called the "equivalent substitution" step.

To investigate the role of the $TiCl_4$, a contrast experiment without the addition of $TiCl_4$ was carried out with the other reaction conditions unchanged. As a result, no film but some floating substance was observed after it reacted for 6 h or even for 12 h (as shown in Figure 5a and b). Closer observation indicates that the products were some flowerlike nanostructures made up of nanorods (Figure 5c and d). The main difference between the results with and without $TiCl_4$ was whether the number of flowerlike nanostructures was large enough to make them interconnect with each other to form a film or not. As the number of the flowerlike nanostructures depends on that of the initially generated TiO_2 nanocrystals, $TiCl_4$ may play an important role in the nucleation of the film floating growth. In this way, if $TiCl_4$ was substituted for another substance that can act as the seeds for the growth of nanorods or promote nucleation during the floating growth process, the generated flowerlike nanostructures would be enough to interconnect with each other to form a film. As fluorine-doped tin oxide (FTO) nanoparticles can be used to epitaxial growth of TiO_2 nanorods,[31] some of them were scratched from a FTO conducting glass and used to replace $TiCl_4$ to conduct a contrast experiment with other conditions unchanged. As a result, a piece of white TiO_2 film was obtained at the gas−liquid interface and the corresponding SEM images are shown in Figure 6, suggesting that it has similar morphologies with the samples in Figure 1. Therefore, $TiCl_4$ may play an important role in increasing the amount of seeds, which ultimately determines whether the formation of the film or just the formation of large numbers of isolated flowerlike nanostructures.

To investigate the role of TBT, contrast experiments without TBT were carried out with other conditions unchanged. As a result, nothing was observed floating at the gas−liquid interface and white deposition was obtained at the bottom. The hydrolysis of TBT can be expressed as

$$Ti(OC_4H_9)_4 + 2H_2O \leftrightarrow TiO_2 + 4C_4H_9OH$$

where C_4H_9OH is slightly soluble in water with smaller density than water and considering the temperature (150−160 °C), the following side reactions may produce insoluble organics so that a floating water−organics interface can be generated at the gas−liquid interface, which can act as a soft template for the growth of flowerlike nanostructures.[22] Therefore, the organics resulting from the hydrolysis of TBT or the side reactions may determine whether the generated TiO_2 nanostructures float or not. To confirm this, another contrast experiment was performed by substituting TBT for butanol with the same number of moles with the other conditions unchanged. As a result, a large piece of floating nanorod film was obtained as expected and the corresponding SEM images (shown in Figure

7) demonstrate that it has similar morphology just as that of the film obtained using TBT. All these experiment results indicate that the hydrolysis product of TBT (C_4H_9OH or other side reaction products) could act as a floating soft template for the floating growth of nanorod films. Therefore, TBT not only acts as a Ti source for the growth of TiO_2, but also provides a soft template for the floating growth of nanorod films. In addition, the floating growth of the nanorod film results from TBT and floating growth process is a self-templated process.

In this part, the important roles of the main reactants are clarified. $TiCl_4$ can increase the number of seeds, which ultimately determines whether the film can form or not. While besides Ti source, TBT can offer a floating soft template by the hydrolysis reaction or its side reactions, which ultimately determines whether the film can float or not.

3.4. A Scenario for Floating Growth of Nanorod Films. Until now, the two key questions for the floating growth of nanorod films are answered, that is, why the film can achieve floating growth and how the film form at the gas−liquid interface. To achieve floating growth, some organics or compounds, such as TBT, that can generate organics are essential. To form a film, enough seeds or something that can promote nucleation is needed.

On the basis of the analysis above, a scenario for the floating growth of nanorod films was developed shown in Scheme 1. According to the scenario, the self-assembly process of large-scale TiO_2 nanorod films at the gas−liquid interface can be described as the following three stages: (1) Fast hydrolysis, nucleation, aggregation, and the formation of water−organics interface; (2) growth of nanorods and formation of nanorod-based flowerlike nanostructures; and (3) interconnection of the nanoflowers to form the film. At the first stage, TiO_2 nanoparticles are generated mainly via forced hydrolysis of $TiCl_4$ at the interface. At the same time, the organics are produced from the hydrolysis of TBT float at the water surface so that a water-organics interface forms at the gas−liquid interface. Nanoparticles are nucleated prior at the interface than in the solution because of the interfacial energy. Because of the strong attractive forces between neighboring nanocrystals, aggregation occurs at the gas−liquid interface. At the second stage, as the process continues, nanorods begin to grow out of the aggregations from the liquid side while there are nonanorods growing from the gas side because of the absence of Ti source. Therefore, after the film forms, one side is plane while the other side is composed of nanorod-based nanoflowers. At the third stage, when the nanorods grow long enough to interconnect with each other, the film based on nanoflower arrays starts to form and gets strong as the reaction continues.

3.5. Development of Other Recipes to Floating Nanorod Films Based on the Above Scenario. According to our scenario, floating growth of TiO_2 nanorod film will be produced when the reaction meets the following key conditions: (1) the formation of water−organics interface during the reaction and (2) enough seeds adsorbed at the interfaces to make the generated nanorods interconnect with each other. To verify whether the inference based on the scenario is correct or not, we have designed two following experiments.

In the first experiment, we replaced TBT with another titanium complex, tetraethyl titanate in the hydrothermal reaction. Typically, 150 uL $TiCl_4$ and 0.5 g tetraethyl titanate was added into the HCl aqueous solution (with the volume ratio of concentrated hydrochloric acid to water 1:1). Then they were reacted at around 150 °C for 12 h. As predicted based on the scenario, a piece of nanorod film was obtained and it had similar morphology with that obtained above (Figure S3, SI).

In the second experiment, we further replaced $TiCl_4$ with FTO nanocrystals and replaced TBT by tetraethyl titanate (TET) at the same time with other conditions unchanged. As a result, a piece of nanorod film was also obtained at the liquid surface with similar morphology (Figure S4, SI).

By this way, the floating growth scenario proposed above is verified, and two other recipes of preparing floating nanorod film were developed. We believe that the floating growth scenario and the recipes developed based on it will open a new way to prepare not only freestanding TiO_2 nanorod films, floating TiO_2 films but also other freestanding semiconductor films.

Until now a series of experiments were carried out to explore the floating growth mechanism of the floating films. All of the above experimental results are summarized in Table 1. They are categorized into four parts: Part A is the floating growth method we developed before; Parts B and C demonstrate the roles of $TiCl_4$ and TBT in the reaction respectively; and Part D shows two new recipes of floating growth of TiO_2 flowerlike film, which are developed based on the growth scenario proposed above.

3.6. Application of the Freestanding Film in Additive-Free Li-Ion Batteries. Titanium dioxide (TiO_2) is an attractive material for Li-ion battery anodes with high safety and stability. However, because of the poor electronic conductivity, large amounts of conducting agent and binder (typical weight ratio of TiO_2, conducting agent, and binder = 80:10:10) are used to improve the conductivity and form a film. As a result, the specific capacity (unit, for example, mAh/g) of the anode is much reduced because the addition of the additives increases the total mass of the anode but not contribute to the charge−discharge capacity. As the free-standing film is large-scale continuous and stable enough so that binder is not essential. Furthermore, as almost all the nanorods have a direct electron transfer path from one side to the other side of the film, the conductivity can be improved so that the elimination of conducting agent may be possible. On the basis of the analysis above, an additive-free TiO_2 anode was fabricated and applied to a CR2032 coin cell.

A typical initial charge−discharge curve is shown in Figure 8a, and the corresponding cycle performance is shown in Figure 8b. The initial discharge areal capacity is 31.44 mAh/g under current density of 30 mA/g. After 100 charge−discharge cycles, the discharge capacity is 32.66 mAh/g without any loss but a little increase. And the good cycle performance may be ascribed to the chemical stability of the material during charge−discharge cycles.[32] To the best of our knowledge, this is the first time that additive-free TiO_2-based anode has been successfully applied to a Li-ion battery with good cycle performance.

4. CONCLUSION

In summary, a self-templated growth scenario was proposed to account for the floating growth of large-scale floating TiO_2 nanorod film at the gas−liquid interface. There are two main factors influencing the formation of floating film: water−organics interface and enough seeds. To achieve floating growth, some organics or compounds that can generate organics are essential; and to form a film, enough seeds or

something that can promote nucleation is necessary. On the basis of the proposed scenario, another two recipes of preparing floating nanorod film were developed. Furthermore, the freestanding TiO_2 film was successfully applied to a Li-ion battery as an additive-free anode for the first time, and the discharge capacity has no loss but a little increase after 100 charge−discharge cycles. This work may pave a new way for the synthesis of freestanding and floating TiO_2 and other semiconductor oxide films, which has great potential not only in basic science but also in the applications such as materials engineering, Li-ion battery, photocatalyst, dye-sensitized solar cell, and flexible electronics.

■ ASSOCIATED CONTENT

Supporting Information

Photographs of the film, XRD pattern of the film, and SEM images of the films synthesized by other recipes and so on. This material is available free of charge via the Internet at http://pubs.acs.org.

■ AUTHOR INFORMATION

Corresponding Authors

*E-mail: wtaosun@pku.edu.cn

*E-mail: lmpeng@pku.edu.cn.

Notes

The authors declare no competing financial interest.

■ ACKNOWLEDGMENTS

This work was supported by the Ministry of Science and Technology (Grants 2011CB933002 and 2012CB932702) and National Science Foundation of China (Grants 61306079, 61171023 and 60871002). We thank Prof. Jingyun Wang and Dr. Xuemei Li for assistance with the transmission electron microscope.

■ REFERENCES

(1) Wang, F.; Seo, J.-H.; Ma, Z.; Wang, X. Substrate-Free Self-Assembly Approach toward Large-Area Nanomembranes. *ACS Nano* **2012**, *6* (3), 2602−2609.

(2) Oregan, B.; Gratzel, M.; Low-Cost, A. High-Efficiency Solar-Cell Based on Dye-Sensitized Colloidal TiO_2 Films. *Nature* **1991**, *353* (6346), 737−740.

(3) Fujishima, A.; Honda, K. Electrochemical Photolysis of Water at a Semiconductor Electrode. *Nature* **1972**, *238* (5358), 37−38.

(4) Armstrong, A. R.; Armstrong, G.; Canales, J.; García, R.; Bruce, P. G. Lithium-Ion Intercalation into TiO_2-B Nanowires. *Adv. Mater.* **2005**, *17* (7), 862−865.

(5) Benkstein, K. D.; Semancik, S. Mesoporous Nanoparticle TiO_2 Thin Films for Conductometric Gas Sensing on Microhotplate Platforms. *Sens. Actuators, B* **2006**, *113* (1), 445−453.

(6) Chen, X.; Mao, S. S. Titanium Dioxide Nanomaterials: Synthesis, Properties, Modifications, and Applications. *Chem. Rev.* **2007**, *107* (7), 2891−2959.

(7) Ai, G.; Sun, W. T.; Gao, X. F.; Zhang, Y. L.; Peng, L. M. Hybrid CdSe/TiO_2 Nanowire Photoelectrodes: Fabrication and Photoelectric Performance. *J. Mater. Chem.* **2011**, *21* (24), 8749−8755.

(8) Ai, G.; Sun, W. T.; Zhang, Y. L.; Peng, L. M. Nanoparticle and Nanorod TiO_2 Composite Photoelectrodes with Improved Performance. *Chem. Commun.* **2011**, *47* (23), 6608−6610.

(9) Xin, X.; Zhou, X.; Wu, J.; Yao, X.; Liu, Z. Scalable Synthesis of TiO_2/Graphene Nanostructured Composite with High-Rate Performance for Lithium Ion Batteries. *ACS Nano* **2012**, *6* (12), 11035−11043.

(10) Du, J.; Qi, J.; Wang, D.; Tang, Z. Facile Synthesis of Au@TiO_2 Core-Shell Hollow Spheres for Dye-sensitized Solar Cells with Remarkably Improved Efficiency. *Energy Environ. Sci.* **2012**, *5* (5), 6914−6918.

(11) Lin, C.-J.; Yu, W.-Y.; Lu, Y.-T.; Chien, S.-H. Fabrication of Open-ended High Aspect-ratio Anodic TiO_2 Nanotube Films for Photocatalytic and Photoelectrocatalytic Applications. *Chem. Commun.* **2008**, *0* (45), 6031−6033.

(12) Chen, Q.; Xu, D. Large-Scale, Noncurling, and Free-Standing Crystallized TiO_2 Nanotube Arrays for Dye-Sensitized Solar Cells. *J. Phys. Chem. C* **2009**, *113* (15), 6310−6314.

(13) Lin, C.-J.; Yu, W.-Y.; Chien, S.-H. Transparent Electrodes of Ordered Opened-End TiO_2-Nanotube Arrays for Highly Efficient Dye-sensitized Solar Cells. *J. Mater. Chem.* **2010**, *20* (6), 1073−1077.

(14) Roy, P.; Dey, T.; Lee, K.; Kim, D.; Fabry, B.; Schmuki, P. Size-Selective Separation of Macromolecules by Nanochannel Titania Membrane with Self-Cleaning (Declogging) Ability. *J. Am. Chem. Soc.* **2010**, *132* (23), 7893−7895.

(15) Liu, Y.; Wang, H.; Wang, Y. C.; Xu, H. M.; Li, M.; Shen, H. Substrate-Free, Large-Scale, Free-Standing and Two-Side Triented Single Crystal TiO_2 Nanorod Array Films with Photocatalytic Properties. *Chem. Commun.* **2011**, *47* (13), 3790−3792.

(16) Liu, Y.; Wang, H.; Li, H. B.; Zhao, W. X.; Liang, C. L.; Huang, H.; Deng, Y. J.; Shen, H. Length-Controlled Synthesis of Oriented Single-Crystal Rutile TiO_2 Nanowire Arrays. *J. Colloid Interface Sci.* **2011**, *363* (2), 504−510.

(17) Zeng, T.; Tao, H. Z.; Sui, X. T.; Zhou, X. D.; Zhao, X. J. Growth of Free-Standing TiO_2 Nanorod Arrays and its Application in CdS Quantum Dots-Sensitized Solar Cells. *Chem. Phys. Lett.* **2011**, *508* (1−3), 130−133.

(18) Xia, H.-R.; Li, J.; Peng, C.; Li, L.-W.; Sun, W.-T.; Peng, L.-M. Self-Assembly of Large-Scale Floating TiO_2 Nanorod Arrays at the Gas−Liquid Interface. *ACS Appl. Mater. Interfaces* **2013**, *5*, 8850−8852.

(19) Xia, H.-R.; Peng, C.; Li, J.; Sun, W.-T.; Ai, G.; Peng, L.-M. Large-Scale Floated Single-Crystalline TiO_2 Flower-like Films: Synthesis Details and Applications. *RSC Adv.* **2013**, *3*, 17668−17671.

(20) Xu, S.; Hessel, C. M.; Ren, H.; Yu, R.; Jin, Q.; Yang, M.; Zhao, H.; Wang, D. α-Fe_2O_3 Multi-Shelled Hollow Microspheres for Lithium Ion Battery Anodes with Superior Capacity and Charge Retention. *Energy Environ. Sci.* **2014**, *7* (2), 632−637.

(21) Phan, T. D. N.; Pham, H. D.; Cuong, T. V.; Kim, E. J.; Kim, S.; Shin, E. W. A Simple Hydrothermal Preparation of TiO_2 Nanomaterials Using Concentrated Hydrochloric Acid. *J. Cryst. Growth* **2009**, *312* (1), 79−85.

(22) Wang, C. H.; Shao, C. L.; Liu, Y. C.; Li, X. H. Water−Dichloromethane Interface Controlled Synthesis of Hierarchical Rutile TiO_2 Superstructures and Their Photocatalytic Properties. *Inorg. Chem.* **2009**, *48* (3), 1105−1113.

(23) Zhang, G. N.; Roy, B. K.; Allard, L. F.; Cho, J. Titanium Oxide Nanoparticles Precipitated from Low-Temperature Aqueous Solutions: II. Thin−Film Formation and Microstructure Developments. *J. Am. Ceram. Soc.* **2010**, *93* (7), 1909−1915.

(24) Sarkar, D.; Ghosh, C. K.; Chattopadhyay, K. K. Morphology Control of Rutile TiO_2 Hierarchical Architectures and Their Excellent Field Emission Properties. *CrystEngComm* **2012**, *14* (8), 2683−2690.

(25) Zhang, G. N.; Roy, B. K.; Allard, L. F.; Cho, J. H. Titanium Oxide Nanoparticles Precipitated from Low-Temperature Aqueous Solutions: I. Nucleation, Growth, and Aggregation. *J. Am. Ceram. Soc.* **2008**, *91* (12), 3875−3882.

(26) Dessombz, A.; Chiche, D.; Davidson, P.; Panine, P.; Chaneac, C.; Jolivet, J.-P. Design of Liquid-Crystalline Aqueous Suspensions of Rutile Nanorods: Evidence of Anisotropic Photocatalytic Properties. *J. Am. Chem. Soc.* **2007**, *129* (18), 5904−5909.

(27) Hosono, E.; Fujihara, S.; Honma, I.; Zhou, H. S. Superhydrophobic Perpendicular Nanopin Film by the Bottom-Up Process. *J. Am. Chem. Soc.* **2005**, *127* (39), 13458−13459.

(28) Liu, S. J.; Gong, J. Y.; Hu, B.; Yu, S. H. Mesocrystals of Rutile TiO_2: Mesoscale Transformation, Crystallization, and Growth by a Biologic Molecules-Assisted Hydrothermal Process. *Cryst. Growth Des.* **2009**, *9* (1), 203−209.

(29) Sun, C.; Wang, N.; Zhou, S.; Hu, X.; Zhou, S.; Chen, P. Preparation of Self-Supporting Hierarchical Nanostructured Anatase/Rutile Composite TiO_2 Film. *Chem. Commun.* **2008**, *28*, 3293−3295.
(30) Hosono, E.; Fujihara, S.; Kakiuchi, K.; Imai, H. Growth of Submicrometer-Scale Rectangular Parallelepiped Rutile TiO_2 Films in Aqueous $TiCl_3$ Solutions Under Hydrothermal Conditions. *J. Am. Chem. Soc.* **2004**, *126* (25), 7790−7791.
(31) Feng, X.; Shankar, K.; Varghese, O. K.; Paulose, M.; Latempa, T. J.; Grimes, C. A. Vertically Aligned Single Crystal TiO_2 Nanowire Arrays Grown Directly on Transparent Conducting Oxide Coated Glass: Synthesis Details and Applications. *Nano Lett.* **2008**, *8* (11), 3781−3786.
(32) Hu, Y. S.; Kienle, L.; Guo, Y. G.; Maier, J. High Lithium Electroactivity of Nanometer-Sized Rutile TiO_2. *Adv. Mater.* **2006**, *18* (11), 1421−1426.